JTE HCMUTE
ISSN: 2615-9740

JOURNAL OF TECHNICAL EDUCATION SCIENCE
Ho Chi Minh City University of Technology and Education
Website: https://jte.edu.vn
Email: jte@hcmute.edu.vn

Preparation and Characterization of 1D, 2D, and 3D Shapes of Anisotropic Gold Nanoparticles

Trong Phat Huynh[2], Hoang Trung Huynh[1*], Duc Trung Vu[1], Dinh Tung Nguyen[1], Thai Gia Phu Pham[1], Thi Hong Tham Nguyen[2]

[1]*Ho Chi Minh City University of Technology and Education, Vietnam*
[2]*Research Laboratories of Saigon Hi-Tech Park, Vietnam*

[*]Corresponding author. *Email: trunghh@hcmute.edu.vn*

ARTICLE INFO

Received: 26/09/2023
Revised: 31/10/2023
Accepted: 27/03/2024
Published: 28/08/2024

KEYWORDS

Anisotropic gold nanoparticles;
Gold nanobipyramids;
Gold nanoprisms;
Gold nanostars;
Seed-mediated method.

ABSTRACT

In recent times, the scientific community has become interested in gold nanoparticles, namely in the anisotropic class. Based on their shapes, they fall into three categories: one-, two-, and three-dimensional. The synthesis and properties of three different anisotropic gold nanoparticle preparations - gold nanobipyramids (one-dimension, 1D), gold nanoprisms (two-dimension, 2D), and gold stars (three-dimension, 3D) - are shown in this research. Here, our group describes a chemical reduction method mediated by seeds. X-ray powder diffraction, transmission electron microscopy, scanning electron microscopy, and ultraviolet-visible spectroscopy were used to analyze the anisotropic gold nanoparticles. The average dimensions of the nanobipyramids were 64.27 ± 7.31 nm for length and 25.87 ± 2.56 nm for diameter, according to the data; the average dimensions of the gold nanoprisms and goldstars were 43.54 ± 5.61 nm and 31.35 ± 7.01 nm, respectively. Furthermore, following centrifugation purification, the yields of triangle and bipyramidal particles rose from 40% to over 60% and from 60% to 90%, respectively. It was established what the ideal parameter concentration was to create anisotropic gold nanoparticles in three dimensions: one, two, and three.

Doi: https://doi.org/10.54644/jte.2024.1457

1. Introduction

Noble metal nanoparticles, especially gold nanoparticles (AuNPs), show special physical and chemical properties that are different from those of their bulk materials [1]. Depending on their shape and properties, gold nanoparticles are classified into two main groups: isotropic and anisotropic. Therein, anisotropic AuNPs have the attracted interest of the scientific community in the last two decades [2]. Because of their advanced unique chemical, physical, and optical properties [3], anisotropic AuNPs have very important and advanced applications in fields including optical and biosensors, biomedicine, and chemical catalysis [4], [5].

Localized surface plasmon is a vibration of free and easily polarizable electrons in noble metals under an exciting electromagnetic wave. Consequently, noble metallic particles with a suitable nanosize will resonate and amplify the frequency of a suitable electromagnetic field. This resonance phenomenon is defined as localized surface plasmon (SPR) [6]. The SPR of isotropic AuNPs, or nanospheres, ranges from 520 to 550 nm. However, depending on the size and shape of the particles, these anisotropic AuNPs show more than two SPR bands, with one absorption at 520 nm to 550 nm and others spanning from 600 nm to over 1200 nm [7]. Transverse surface plasmon resonance (TSPR) is the peak in the blue shift (520-550 nm), and longitudinal surface plasmon resonance (LSPR) is the absorbances in the near-infrared region [8].

Although there are many techniques to synthesize anisotropic AuNPs, such as chemical reduction, electrochemistry, irradiation, sonochemistry, solvothermal, photochemistry, and laser ablation methods [9], seed-mediated growth is still the main process to prepare anisotropic AuNPs [10]. Chemical reduction is a rapid and simple method for anisotropic AuNPs; however, a few types, such as multi-

branched or plate nanoparticles, are formed, obtaining a small and polydisperse size. Electrochemistry is a different way of synthesizing anisotropic AuNPs. The advantage of this method is its high purity. However, this technique is involuntary, as only nanorods can be obtained. Other procedures are photochemistry and sonochemistry. These methods are “green chemistry," so they have attracted attention in recent years. But low yields and complicated equipment are their disadvantages. Among methods for the preparation of anisotropic AuNPs, seed-mediation is one of the most effective procedures. This technique includes two stages: seed formation and anisotropic growth. Besides, the morphology and size of anisotropic AuNPs can be controlled by adjusting shaped-directing and reduced agents.

In this work, we report the preparations of three anisotropic AuNPs classified as 1D gold nanobipyramids (NBPs), 2D gold nanoprimes (AuNPrs), and 3D gold nanostars (GNS) by a seed-mediated growth process in high yield. Moreover, the effects of ascorbic acid, $AgNO_3$, surfactant concentration, and pH on the morphology and size of their shaped-directing agents (surfactants and $AgNO_3$), reduced agents, and pH on morphology and size were characterized using ultraviolet-visible spectroscopy (UV-Vis), scanning electron microscopy (SEM), transmission electron microscopy (TEM), and X-ray powder diffraction (XRD). Finally, the average particle sizes were calculated by Image-J software based on TEM micrographs.

2. Materials and Methods

2.1. Materials

Tetrachloroauric (III) acid ($HAuCl_4.xH_2O$, 52%), triton X-100, cetyltrimethylammonium chloride (CTAC, solution 25%), cetyltrimethylammonium bromide (CTAB, 99%), sodium borohydride ($NaBH_4$, 99%), silver nitrate ($AgNO_3$, 99%), and sodium hydroxide (NaOH, 98%) were purchased from Sigma-Aldrich. Ascorbic acid and sulfuric acid (H_2SO_4, 99%) were obtained from VWR Chemicals. Potassium iodide (KI, 99%) was supplied by Guangdong Guanghua Sci-Tech. De-ionic water was used throughout the experiments. All chemical materials were GR-grade.

2.2. Methods

2.2.1. Synthesis of the seed solutions

As per a prior publication [10], the process of preparing CTAB-stabilized gold nanoparticles (seeds) was altered. First, at room temperature, 50 µl of 0.01M $HAuCl_4$ was combined with 1 ml of 0.2M CTAB solution and 950 µl DI water while stirring. Next, 200 µl of a cold (4 ^oC) freshly prepared 0.1M $NaBH_4$ solution was added immediately to this mixture. The solution changed from orange to brownish yellow, indicating seed particle formation. This solution was kept at room temperature for at least 24 hours for the next experiments.

2.2.2. Preparation of anisotropic AuNPs

Preparation and purification of gold nanobipyramids (NBPs): The procedure for the synthesis of NBPs was shown as follows: 250 µl of aqueous 0.01M $HAuCl_4$ was added to 2.5 ml of 0.2M CTAB solution and 2.25 ml DI water under stirring. The mixture turned brownish-yellow. Besides, 37.5 µl of ascorbic acid (AA) 0.1M was added to the brownish-yellow solution above. This mixture immediately changed from brownish-yellow to colorless. After that, 50 µl of aqueous 0.01M $AgNO_3$ solution was dissolved in the mixture solution and the pH was adjusted to about 3 using H_2SO_4 at 20%. Next, this solution was dissolved in 17.5 µl of the seed solutions at room temperature for at least 5 hours. The solution changed from no color to ruby red, indicating NBPs formation.

Preparation and purification of gold nanoprisms (AuNPrs): The mixture contained 250 µl of 0.01M $HAuCl_4$, 2.5 ml of aqueous 0.1M CTAC solution, 42.5 µl of 0.1M KI, and 2.25 ml of DI water. Then, 70 µl of AA 0.1M was added to the mixture above. This mixture immediately changed from a slight yellow to colorless. Next, a NaOH 0.1M solution was used to adjust the pH to about 3. Finally, 57.5 µl of the seed solution was dissolved in this mixture at room temperature for at least 5 hours. The mixture changed from colorless to blue, indicating AuNPrs formation.

Preparation and purification of gold nanostars (GNS): 250 µl of aqueous 0.01M $HAuCl_4$ and 1.0 ml of 0.2M Triton X-1-00 were added to 3.75 ml of DI water. Next, 30.0 µl of 0.01M $AgNO_3$ was added to this mixture. Additionally, 250.0 µl of AA 0.1M was mixed in this solution. This solution immediately changed to colorless. Finally, 75.0 µl of seed solution was dissolved in the solution above at room temperature for about 5 hours. The solution changed from colorless to cobalt, indicating GNS formation.

2.2.3. Purification of anisotropic AuNPs

Using centrifugation, the generated anisotropic AuNPs were refined to eliminate any remaining CTAB and gold nanospheres. The following procedure was followed in order to purify the anisotropic AuNPs that were produced: NBPs, GNS, and AuNPrs anisotropic AuNPs were each subjected to a 5-minute centrifugation at 2000 rpm. To be used again, the precipitants were redispersed in DI water.

2.2.4. Characterization of anisotropic AuNPs

The spectroscopic behaviors for anisotropic AuNPs were recorded using a UV-Vis spectrophotometer (Jasco V-730). The micrographs of anisotropic AuNPs were carried out by scanning electron microscopy (SEM, Hitachi S-4800) and transmission electron microscopy (JEM1010-JEOL). X-ray diffraction (XRD, Bruker D5005 diffractometer) was employed to characterize the structure of anisotropic AuNPs.

3. Results and Discussion

3.1. Effect of surfactants on formation of anisotropic AuNPs

An absorption spectrometer and SEM were used to examine the impact of surfactant on the creation of NBPs (Figure 1). Figure 1a. displays the absorption spectrum of NBPs in this instance. The two peaks at 540 nm (TSPR) and 793 nm (LSPR) could clearly be seen. In addition, the LSPR to TSPR ratio at a 0.05M CTAB concentration was 1.9. At 0.1M CTAB, the TSPR peak was at 531 nm, and the LSPR peak had moved to 752 nm. The maximum SPR decreased, while the LSPR to TSPR ratio reached the highest value 3.6. While the ratio of LSPR to TSPR steadily decreased in response to rising CTAB concentrations at 0.15M, the LSPR shifted into the NIR region. SEM micrographs of NBPs produced at 0.1M CTAB are displayed in Figure 1b. The produced NBPs had a high degree of shape homogeneity and were clearly less polluted. Thus, the best concentration to create uniformly bipyramidal gold nanoparticles might be 0.1M CTAB.

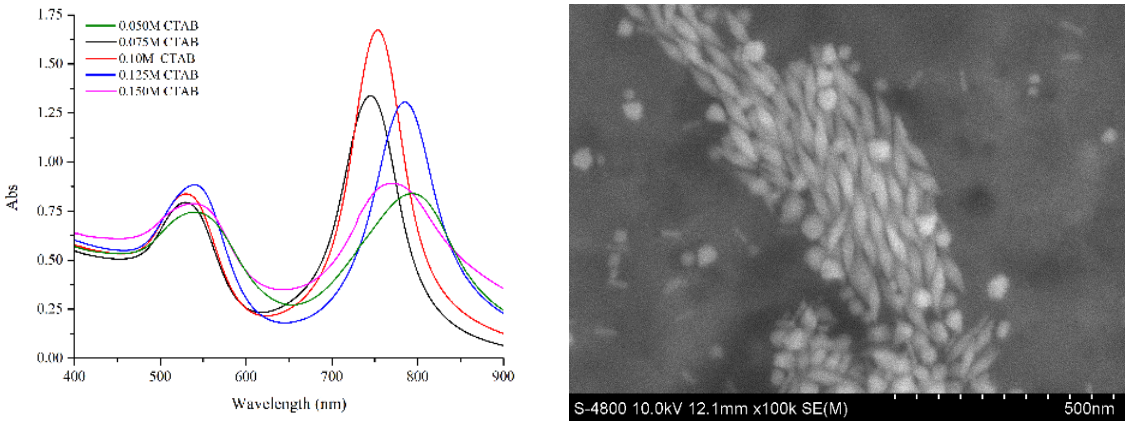

(a) *(b)*

Figure 1. *(a) UV-Vis spectra and (b) SEM micrograph of NBPs synthesized at different CTAB concentrations*

CTAC is the surfactant for the preparation of AuNPrs. The characterization of AuNPrs synthesized at various CATC concentrations is shown in Figure 2. It was clear that the absorption spectra of AuNPrs synthesized at 0.02M CTAC exhibited only one peak at 542 nm, indicating that only spheres were produced. Kept on increasing to 0.03M CTAC and 0.04M CTAC, the UV-Vis spectrum resulted in two absorbances, including one band at 559 nm (TSPR) and 620 nm (LSPR). It was noticeable that the ratios of LSPR to TSPR were trivial. The UV-Vis absorption of AuNPrs synthesized at 0.05M CTAC

illustrated two clear TSPR peaks at 537 nm and LSPR at 627 nm. Moreover, the ratio of LSPR to TSPR was intense. However, the absorbance showed only one wide band ranging from 522 nm to 617 nm when increasing CTAC concentration to 0.06M (Figure 2a). Furthermore, based on the SEM micrographs displayed in Figure 2b, AuNPrs produced at 0.05M obtained a homogenous shape and average size. It could be determined that 0.05M CTAC was the best concentration to create AuNPrs.

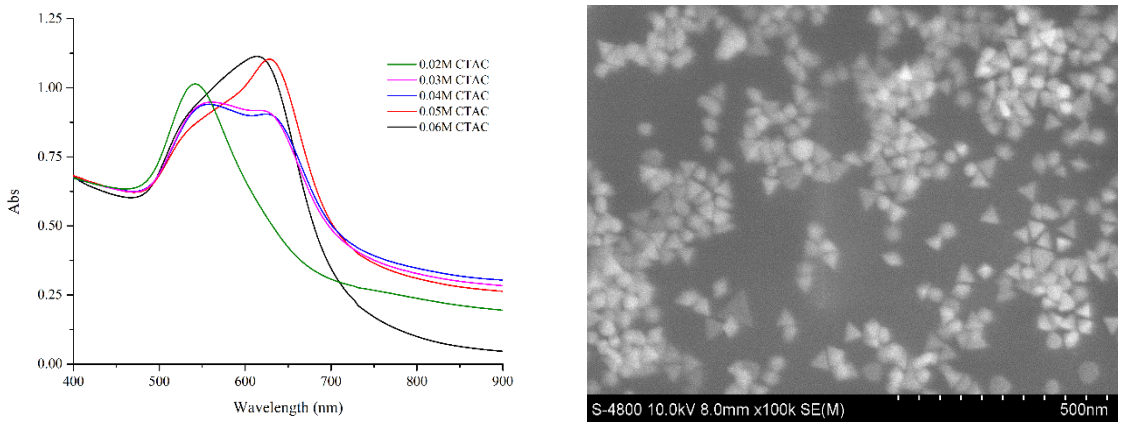

(a) *(b)*

Figure 2. *(a) UV-Vis spectra and (b) SEM micrograph of AuNPrs synthesized at different CTAC concentrations*

Triton X-100 was used as a surfactant for the synthesis of GNS. The investigated effect of Triton X-100 on GNS formation is shown in Figure 3. The UV-Vis results in Figure 3a illustrate the wide broadbands ranging from 600 nm to 950 nm corresponding to the SPR of GNS's tips. The intensity of SPR rose and reached its highest value at 0.02M Triton X-100. In contrast, the SPR's intensity declined when increasing Triton X-100 concentrations. At 0.04M Triton X-100, homogeneous multi-branched gold nanoparticles were visible in the micrograph shown in Figure 3b.

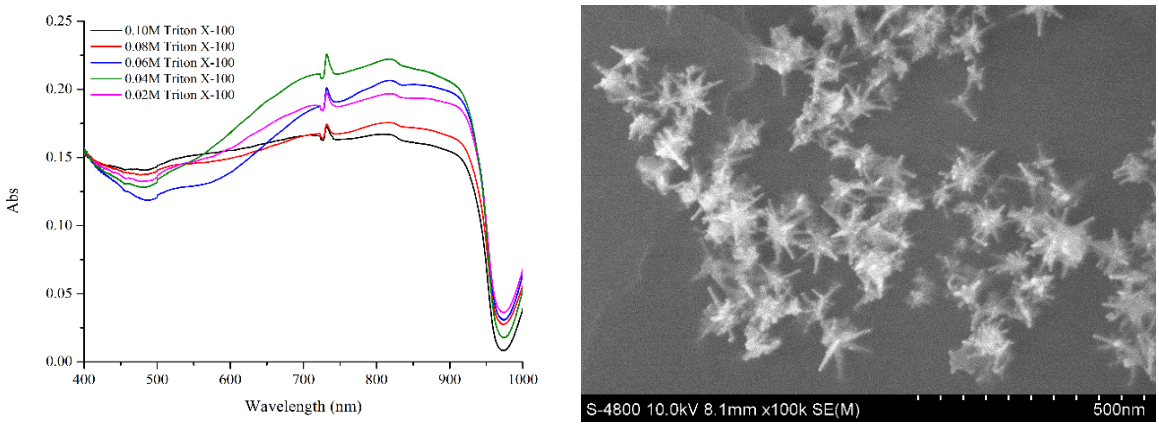

(a) *(b)*

Figure 3. *(a) UV-Vis spectra and (b) SEM micrograph of GNS synthesized at different Triton X-100 concentrations*

3.2. Effect of shaped-directing agents on formation of anisotropic AuNPs

The role of $AgNO_3$ in the preparation of NBPs or GNS is as a shape-directing agent [11], [12]. Figure 4 shows UV-Vis results and an SEM micrograph of NBPs produced in different 0.01M $AgNO_3$ volumes. It was noticeable that only spherical gold nanoparticles formed in the absence of 0.01M $AgNO_3$, according to the absorption spectra. In the presence of 0.01M $AgNO_3$, the UV-Vis results exhibited TSPR's peaks at 550 nm and LSPR peaks in the NIR region. The LSPR was located at 825 nm, and the ratio of LSPR to TSPR was 2.1 at 25 µl of 0.01M $AgNO_3$, followed by an increase of the ratio to 2.8 at 50 µl of 0.01M $AgNO_3$. The ratio reached its highest value at 75 µl of 0.01M $AgNO_3$, and LSPR was located at 805 nm. Both the ratio and location of maximum SPR declined by 2.5 and 787 nm,

respectively, when continuously increasing the volume of 0.01M $AgNO_3$ to 100 µl (Figure 4a). Besides, SEM micrographs of NBPs prepared at 75 µl of 0.01M $AgNO_3$ showed homogeneity and high yield (Figure 4b).

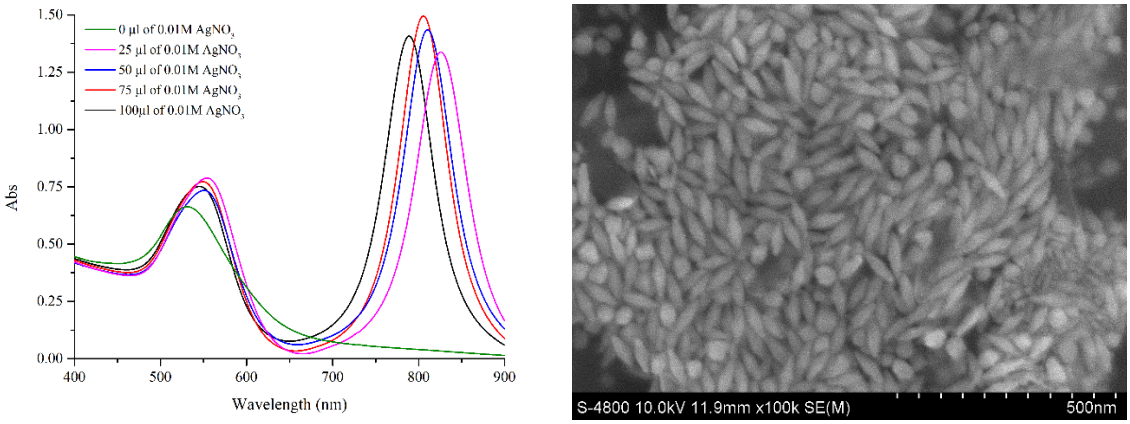

(a) *(b)*

Figure 4. *(a) UV-Vis spectra and (b) SEM micrograph of NBPs synthesized at different 0.01M $AgNO_3$ volumes*

In the synthesis of AuNPrs, KI plays a role as a shape-directing agent. The maximum SPR of prepared AuNPrs shifted from 606 nm to 611 nm while the intensity increased in 40.0 µl of 0.01M KI, but both absorption location and intensity declined as the volume of 0.01M KI increased to 45 µl (Figure 5a). Moreover, the SEM micrograph in Figure 5b indicated uniform shapes of AuNPrs synthesized at 40.0 µl of 0.01M KI. These could be determined with 40.0 µl of 0.01M KI suitably to prepare AuNPrs.

Like NBPs, $AgNO_3$ plays a role as a shape-directing agent to form multi-branches. The UV-Vis and SEM investigations of prepared GNS in various 0.01M $AgNO_3$ volumes are shown in Figure 6. Herein, the absorption spectrum results in Figure 6a showed wide, broad bands ranging from 550 nm to 950 nm, corresponding to the SPR of GNS's tips. The intensity of SPR increased and reached its highest value at 30 µl of 0.01M $AgNO_3$. However, the SPR's intensity decreased when kept at increasing volumes of 0.01M $AgNO_3$. Furthermore, the SEM micrograph in Figure 6b illustrates GNS with long multi-branches at 30 µl of 0.01M $AgNO_3$ volume.

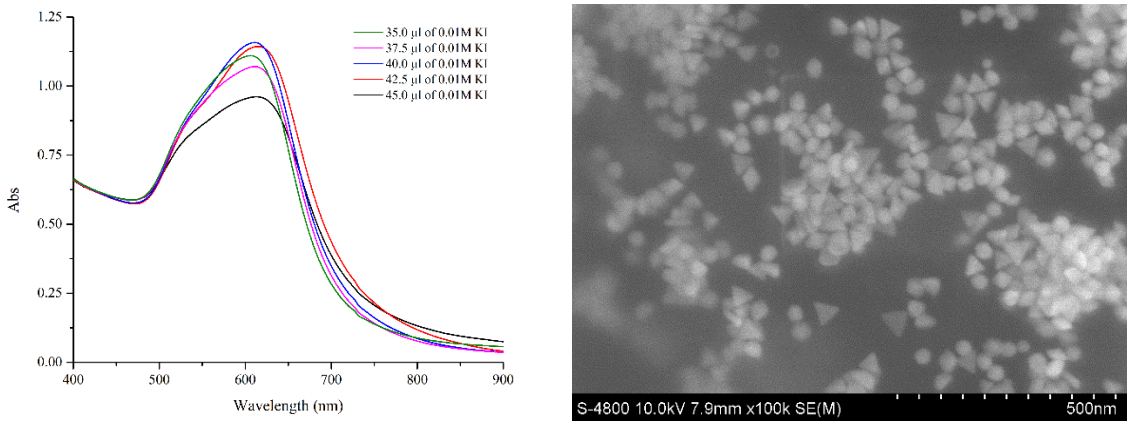

(a) *(b)*

Figure 5. *(a) UV-Vis spectra and (b) SEM micrograph of AuNPrs synthesized at different 0.01M KI volumes*

The role of Ag^+ as a shape-directing agent in the preparation of NBPs and GNS could be explained according to previous reports [12], [13]. The Au seeds are penta-twinned crystals. Silver is indeed not reducible in an acidic solution for the synthesis of NBPs. However, a monolayer or sub-monolayer of Ag can be formed onto Au (110) and Au (100) because of the underpotential deposition (UPD) phenomenon. These sub-monolayers protect the facet from further growth. The ratio of growth rates between Au{100} < Au{110} < Au{111} leads to the unique shape of the bipyramid. In the case of GNS preparation, a monolayer of silver atoms stabilizes the underlying gold atoms on the side wall of

the spiked Au seed particles in the presence of Ag^+ ions. This leads to Au^+ ions interacting on the tips of spikes, which prolongs the length of spikes.

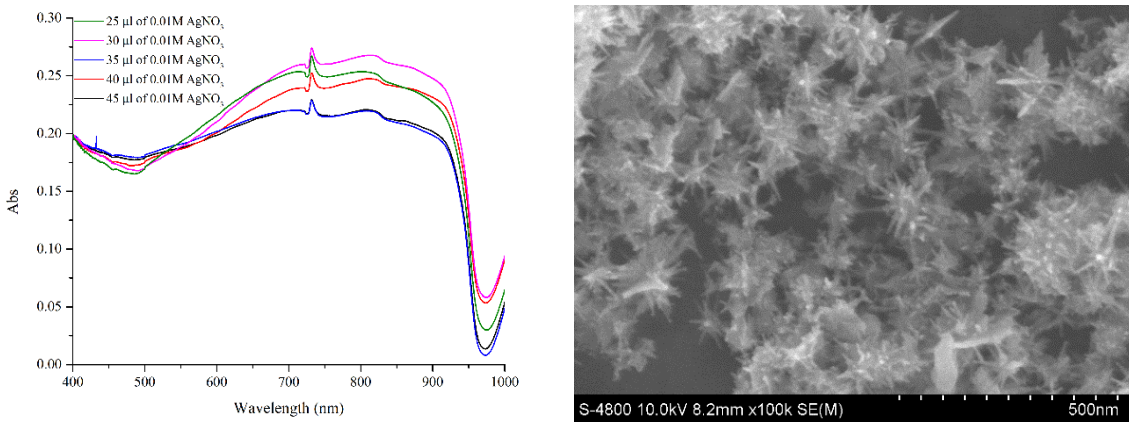

(a) *(b)*

Figure 6. *(a) UV-Vis spectra and (b) SEM micrograph of GNS synthesized at different 0.01M $AgNO_3$ volumes*

The role of the shape-directing agent I- for the preparation of AuNPrs is similar to that of Ag^+ ions. An iodide adlayer binding strongly to Au{100} > Au{110} > Au{111} leads to restricting growth in {100} facets and prior growth in {111} facets [14].

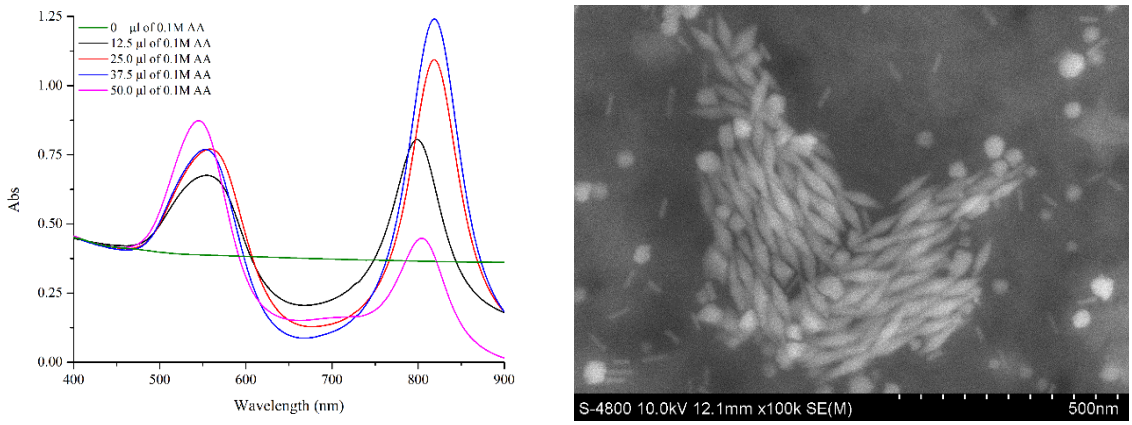

(a) *(b)*

Figure 7. *(a) UV-Vis spectra and (b) SEM micrograph of NBPs synthesized at different 0.1M AA volumes*

3.3. Effect of AA on formation of anisotropic AuNPs

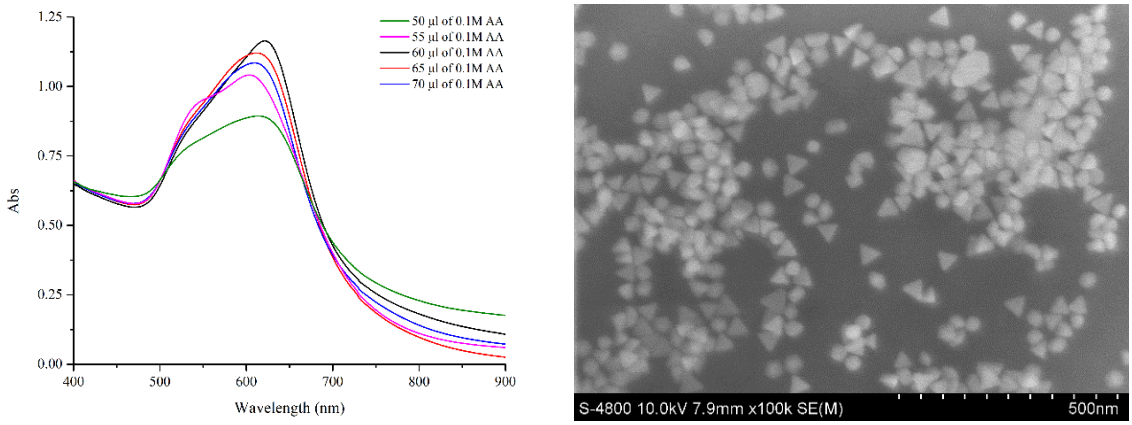

(a) *(b)*

Figure 8. *(a) UV-Vis spectra and (b) SEM micrograph of AuNPrs synthesized at different 0.1M AA volumes*

AA plays an important role in the formation of anisotropic AuNPs. Figure 7 shows the results of UV-Vis and SEM investigations of NBPs synthesized in different 0.1M AA. It was clear that there was an absorption peak in the absence of AA, indicating that the formation of AuNPs did not happen. The LSPR shifted from 798 nm to 818 nm, while the ratio of LSPR to TSPR increased from 1.77 to 2.17 when increasing the volume of 0.1M AA from 12.5 µl to 37.5 µl. Nevertheless, both LSPR absorbance and ratio dropped to 804 nm and 0.65 at 50 µl volume of 0.1M AA (Figure 7a). It can be explained that in the absence of AA, Au^{3+} ions were not reduced to Au^{0} atoms. However, Au^{3+} ions can be reduced rapidly to spherical gold nanoparticles if the AA concentration is too high [15]. The SEM micrograph in Figure 7b illustrates that NBPs, which were produced at 37.5 µl of 0.1M AA, obtained a high uniform shape and size.

Figure 8 shows the absorption result and SEM micrograph of AuNPrs produced in various 0.1M AA. The SPR shifted from 614 nm to 620 nm, while the intensity of the SPR significantly increased to the highest value when increasing the volume of 0.1M AA from 50 to 60 µl. In contrast, the SPR moved to blueshift at 611 nm, while intensity declined when increasing the volume of 0.1M AA to 70 µl (Figure 8a). Moreover, the SEM micrograph in Figure 8b exhibited a homogeneous triangle shape of AuNPrs synthesized in 70 µl of 0.1M AA.

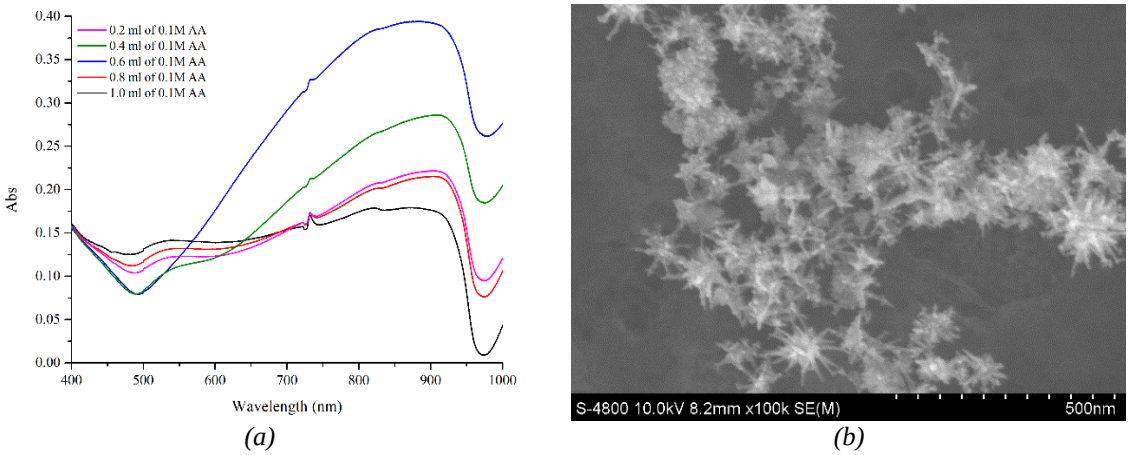

(a) *(b)*

Figure 9. *(a) UV-Vis spectra and (b) SEM micrograph of GNS synthesized at different 0.1M AA volumes*

Figure 9a illustrates the UV-Vis results of GNS prepared in different volumes of 0.1M. It was noticeable that the intensity of maximum SPR located at 903 nm significantly rose when increasing the volume of 0.1M AA from 0.2 ml to 0.6 ml. However, the intensity of max SPR decreased rapidly at a higher volume of 0.1M AA. Figure 9b shows the SEM micrograph of the GNS prepared at 0.6 ml of AA, with length, uniformity, and multi-branches on the whole surface of the AuNPs.

3.4. Purification of anisotropic AuNPs

The characterized results of produced and purified anisotropic AuNPs are exhibited in Figure 10. The UV-NIR absorption spectrum in Figure 10a illustrated the decrease of the full width at half maximum (FWHM) of purified NBPs, indicating that purified NBPs were more homogeneous than produced NBPs [16]. SEM micrographs of produced NBPs and purified NBPs are shown in Figure 10b and 10c, respectively. It was clear that there were many contaminating particles, such as spheres or rods, in the produced NBPs, while contaminating particles were removed in the purified NBPs. Consequently, the yield of bipyramidal particles was increasing from 60% to over 90%, based on SEM micrographs. Besides, the UV-Vis showed that the FWHM of purified AuNPr was narrower than that of produced AuNPrs (Figure 10d). The micrographs in Figure 10e and 10f also indicated that the yield of triangle particles increased from 40% to 60%.

The average size of anisotropic AuNPs were measured using ImageJ software based on TEM micrographs (Figure 11) [17]. According to the results, the average size of NBPs was 64.27 ± 7.31 nm in length and 25.87 ± 2.56 nm in diameter. Moreover, the average size of AuNPrs and GNS were 43.54 ± 5.61 and 31.35 ± 7.01 nm, respectively.

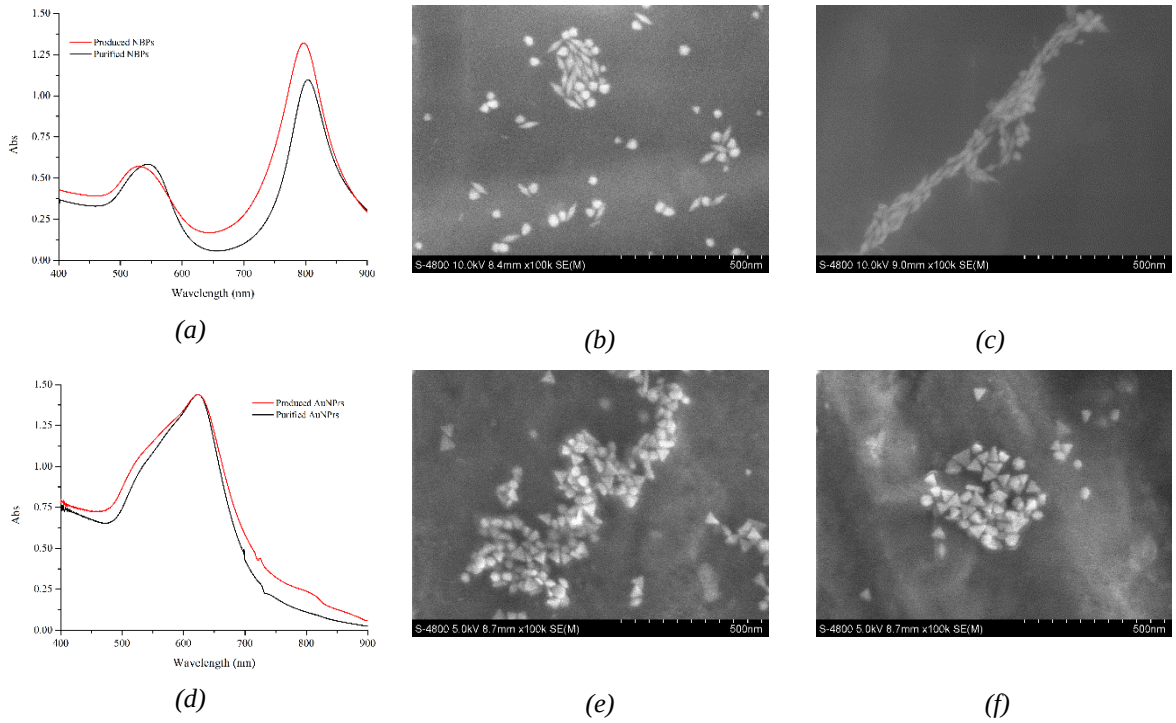

(a) *(b)* *(c)*

(d) *(e)* *(f)*

Figure 10. *(a) UV-Vis spectra of purified NBPs; (b) SEM micrograph of produced NBPs; (c) SEM micrograph of purified NBPs; (d) UV-Vis spectra of purified AuNPrs; (e) SEM micrograph of produced AuNPrs; and (f) SEM micrograph of purified AuNPrs*

Figure 12 shows the mapping energy-dispersive X-ray spectroscopy (EDX) of NBPs, AuNPrs, and GNS spectra. All results revealed a strong peak at 2 keV, indicating the presence of gold elements (except the Cu element of copper grids and the Al element of SEM stub).

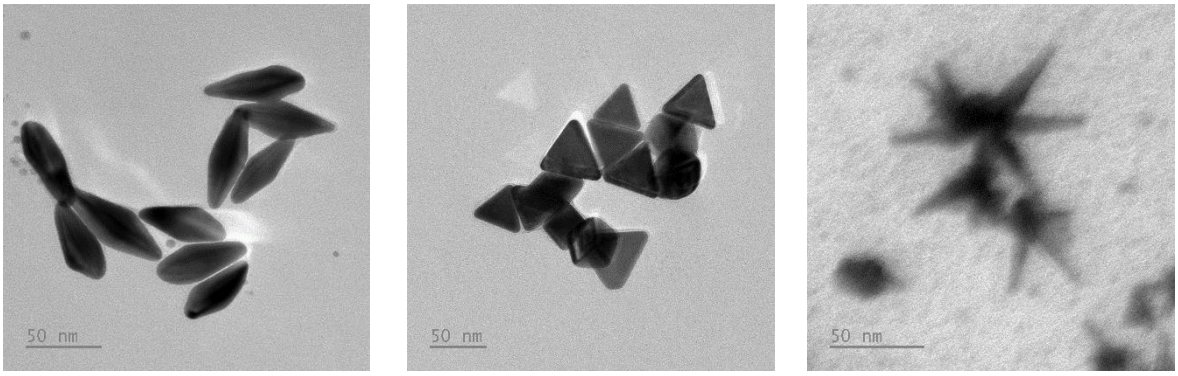

(a) *(b)* *(c)*

Figure 11. *TEM micrographs of (a) NBPS; (b) AuNPrs and (c) GNS*

Figure 13 shows the XRD diffraction patterns of anisotropic AuNPs. The patterns exhibited peaks located at 38.2°, 44.3°, 64.2°, and 78.6°, which correspond to the (111), (200), (220), and (311) planes of the gold face-centered-cubic (fcc) crystalline structure, respectively [18]. According to ICDD card No. 03-065-2870 as the standard reference for the AuNPs [19], the intense peak is located at 38.2, indexing to the (111) plane. Moreover, the (220) plane exhibits a stronger peak at 64.2°, while the (200) plane has a smaller peak at 44.3°. Lastly, the 311 plane is connected to a delicate peak at 78.6°. It was observed that the peak associated with the (111) plane of NBPs (Figure 11a) was the strongest, whilst the peak associated with the (111) plane of AuNPrs was moderately intense and the peak associated with GNS was the weakest (Figures 11b and 11c).

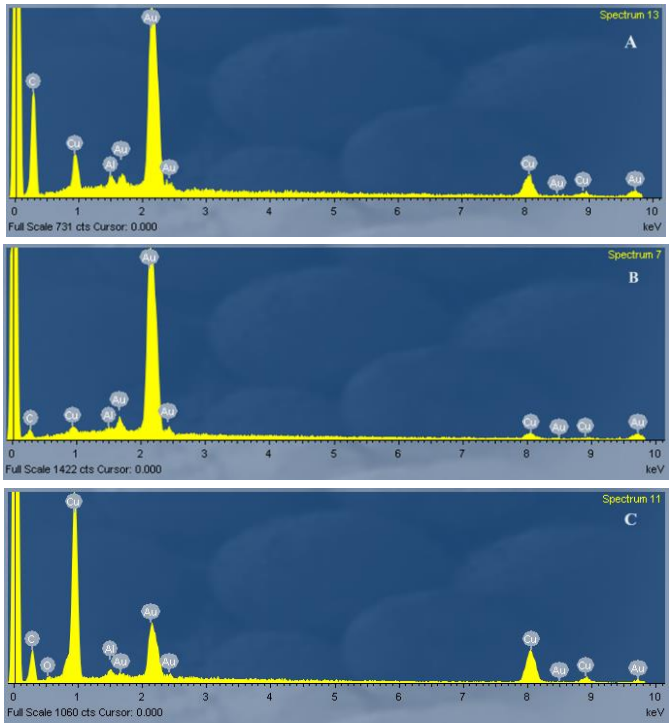

Figure 12. *EDX spectrum of (A) NBPs; (B) AuNPrs and (C) GNS*

This can be explained by the fact that NBPs have ten {111} facets with a penta-twinned crystalline structure [20], [21], whereas AuNPrs just have two {111} facets [22], [23]. Additionally, the peak corresponds to the {111} facets of GNS, which are the result of spots on tips diffraction covering the entire particle surface [24]. The intensity of the peak matched the (111) plane of NBPs, which was the most intense, due to the highest density of {111} facets.

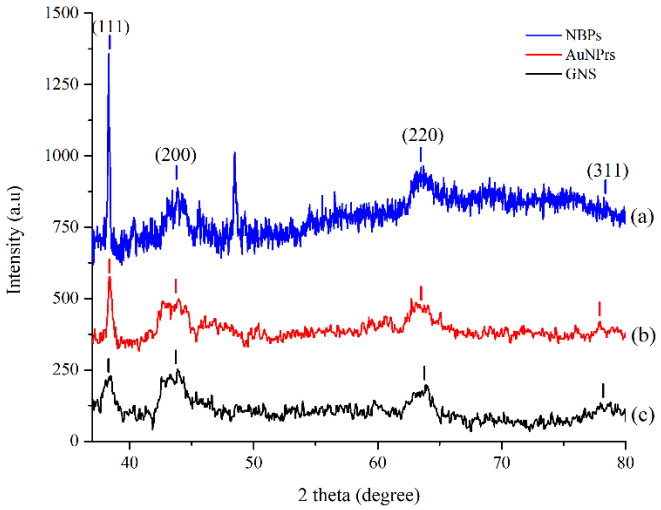

Figure 13. *XRD patterns of (a) NBPS; (b) AuPrs and (c) GNS*

4. Conclusions

This article describes the use of a seed-mediated technique to generate 1D, 2D, and 3D anisotropic AuNPs, such as NBPs, AuNPrs, and GNS. The impact of factors on the size and morphology of anisotropic AuNPs were examined using characterisation techniques such electron microscopy, XRD, and absorption spectra. There, GNS is made using Triton X-100 surfactant, and NBPs and AuNPrs are synthesized using CTAB. Additionally, AgNO3 directs the form of NBPs and GNS synthesis, while KI is involved in the synthesis of AuNPr. Each type of anisotropic AuNP was found to be uniform in size

and shape based on the data obtained from SEM and TEM micrographs. Consequently, the best synthesis parameters for AuNPrs, GNS, and NBPs were identified. Furthermore, NBPs with a high density of {111} facets can serve as antibacterial materials in place of antibiotics. Additionally, AuNPrs and GNS, which show NIR surface plasmon resonance absorbances, may find use in optical sensors.

Acknowledgments

The laboratories and facilities utilized in this paper were provided by the Laboratories of Saigon Hi-Tech, for which the authors are thankful.

Additionally, Saigon Hi-Tech Park (HCM) provided financial support for the materials and chemical agents utilized in this work under decision numbers 17/QĐ-KCNC on February 1st, 2023, and grand number 01/2023/HĐ-TTR&D on February 10th, 2023.

Conflict of Interest

The authors declare no conflict of interest.

REFERENCES

[1] H. Hassan, P. Sharma, M. R. Hasan, S. Singh, D. Thakur, and J. Narang, "Gold nanomaterials – The golden approach from synthesis to applications," *Materials Science for Energy Technologies*, vol. 5, pp. 375-390, 2022.
[2] J. E. O. Castillo, R. C. G. Villanueva, M. J. Madou, and V. H. P. Gonzalez, "Anisotropic gold nanoparticles: A survey of recent synthetic methodologies," *Coordination Chemistry Reviews*, vol. 425, p. 213489, 2020.
[3] C. Xue and Q. Li, "Anisotropic Nanomaterials," in *Anisotropic Nanomaterials: Preparation, Properties, and Applications*, Q. Li, Ed.: Springer International Publishing, 2015, pp. 69-118.
[4] G. Paramasivam, N. Kayambu, A. M. Rabel, A. K. Sundramoorthy, and A. Sundaramurthy, "Anisotropic noble metal nanoparticles: Synthesis, surface functionalization and applications in biosensing, bioimaging, drug delivery and theranostics," *Acta Biomaterialia*, vol. 49, pp. 45-65, 2017.
[5] H. Malekzad, P. S. Zangabad, H. Mirshekari, M. Karimi, and M. R. Hamblin, "Noble metal nanoparticles in biosensors: recent studies and applications," *Nanotechnology Reviews*, vol. 6, no. 3, pp. 301-329, 2017.
[6] C. Kohout, C. Santi, and L. Polito, "Anisotropic Gold Nanoparticles in Biomedical Applications," *International Journal of Molecular Sciences*, vol. 19, no. 11, p. 3385, 2018.
[7] P. R. Sajanlal, T. S. Sreeprasad, A. K. Samal, and T. Pradeep, "Anisotropic nanomaterials: structure, growth, assembly, and functions," *Nano Reviews*, vol. 2, no. 1, p. 5883, 2011.
[8] M. Sovizi and M. Aliannezhadi, "Localized surface plasmon resonance (LSPR) of coupled metal nanospheres in longitudinal, transverse and three-dimensional coupling configurations," *Optik*, vol. 252, p. 168518, 2022.
[9] M. Iqbal *et al.*, "Preparation of gold nanoparticles and determination of their particles size via different methods," *Materials Research Bulletin*, vol. 79, pp. 97-104, 2016.
[10] Y. Xia, K. D. Gilroy, H. C. Peng, and X. Xia, "Seed-Mediated Growth of Colloidal Metal Nanocrystals," *Angewandte Chemie International Edition*, vol. 56, no. 1, pp. 60-95, 2017.
[11] D. Chateau *et al.*, "From gold nanobipyramids to nanojavelins for a precise tuning of the plasmon resonance to the infrared wavelengths: experimental and theoretical aspects," *Nanoscale*, vol. 7, no. 5, pp. 1934-1943, 2015, doi: 10.1039/C4NR06323F.
[12] S. Atta, M. Beetz, and L. Fabris, "Understanding the role of AgNO3 concentration and seed morphology in the achievement of tunable shape control in gold nanostars," *Nanoscale*, vol. 11, no. 6, pp. 2946-2958, 2019, doi: 10.1039/C8NR07615D.
[13] M. Liu and P. G. Sionnest, "Mechanism of Silver(I)-Assisted Growth of Gold Nanorods and Bipyramids," *The Journal of Physical Chemistry B*, vol. 109, no. 47, pp. 22192-22200, 2005.
[14] M. Sun, G. Ran, Q. Fu, and W. Xu, "The effect of iodide on the synthesis of gold nanoprisms," *Journal of Experimental Nanoscience*, vol. 10, no. 17, pp. 1309-1318, 2015.
[15] C. Fang, G. Zhao, Y. Xiao, J. Zhao, Z. Zhang, and B. Geng, "Facile Growth of High-Yield Gold Nanobipyramids Induced by Chloroplatinic Acid for High Refractive Index Sensing Properties," *Scientific Reports*, vol. 6, no. 1, p. 36706, 2016.
[16] M. A. Dheyab *et al.*, "Monodisperse Gold Nanoparticles: A Review on Synthesis and Their Application in Modern Medicine," *International Journal of Molecular Sciences*, vol. 23, no. 13, doi: 10.3390/ijms23137400.
[17] N. L. Razali *et al.*, "Formation of anisotropic gold nanoparticles on indium tin oxide substrates as a plasmonic sensing material," *Nanomaterials and Nanotechnology*, vol. 10, p. 1847980420965388, 2020.
[18] K. Pussi *et al.*, "Structural Properties of Nanometer-Sized Gold Nanoparticles on a Silicon Substrate," *physica status solidi (b)*, vol. 259, no. 7, p. 2100572, 2022.
[19] A. S. Abed, Y. H. Khalaf, and A. M. Mohammed, "Green synthesis of gold nanoparticles as an effective opportunity for cancer treatment," *Results in Chemistry*, vol. 5, p. 100848, 2023.
[20] S. Yougbaré *et al.*, "Facet-dependent gold nanocrystals for effective photothermal killing of bacteria," *Journal of Hazardous Materials*, vol. 407, p. 124617, 2021.
[21] A. Mehere and N. B. Chaure, "Precisely controlled shape and size of gold nanostructures by seed-mediated reduction reaction method," *Applied Physics A*, vol. 126, no. 8, p. 662, 2020.
[22] H. A. Keul, M. Möller, and M. R. Bockstaller, "Selective exposition of high and low density crystal facets of gold nanocrystals using the seeded-growth technique," *CrystEngComm*, vol. 13, no. 3, pp. 850-856, 2011, doi: 10.1039/C0CE00267D.
[23] A. R. Tao, S. Habas, and P. Yang, "Shape Control of Colloidal Metal Nanocrystals," *Small*, vol. 4, no. 3, pp. 310-325, 2008.
[24] Q. K. Vo, A. T. Nguyen, H. T. Ho, L. T. N. Huynh, T. P. P. Nguyen, and T. H. T. Nguyen, "Environmentally Friendly Controlled Synthesis of Gold Nanostars with Collagen by One-Step Reduction Method," *Journal of Nanomaterials*, vol. 2022, p. 4046389, 2022.

Huynh Trong Phat is Ph.D. student in Physics and Engineering Physics Faculty of University of Science, VNUHCM. He received B.S. degree (2007) and M.S. degree (2019) in Faculty of Materials Science and Technology, University of Science, VNUHCM. From 2007 to now (2023), he is the researcher at Semiconductor Laboratory, Laboratories of Saigon Hi-tech Park. His research focuses on noble metallic nanoparticles and their application in biosensors and biomedical materials.
Email: htphat.shtp@tphcm.gov.vn. ORCID: https://orcid.org/0000-0003-4706-0062

Huynh Hoang Trung received a master's degree in science from Ho Chi Minh City National University in 2008. He has worked with electronic components such as transistors and UV light-emitting diodes before, and his work has appeared in national and international journal publications. In addition, he has experience with a range of deposition methods, such as sol-gel, chemical vapor deposition, thermal evaporation, and sputtering, for fabricating thin films. Currently, he works as a lecturer at the Ho Chi Minh City University of Technology and Education. Email: trunghh@hcmute.edu.vn.
ORCID: https://orcid.org/0009-0003-1358-6872

Vu Duc Trung was on April 1st, 2001. He is student in Faculty of Applied Sciences, Ho Chi Minh City University of Technology and Education. His thesis is preparation of gold nanobipyramids and application as antibacterial material.
Email: 19130054@student.hcmute.edu.vn. ORCID: https://orcid.org/0009-0006-8537-933X

Nguyen Dinh Tung was on Sep 23rd, 2001. He is student in Faculty of Applied Sciences, Ho Chi Minh City University of Technology and Education. His thesis is synthesis of gold nanoprism and its application in biosensor for glucose detection.
Email: 19130056@student.hcmute.edu.vn. ORCID: https://orcid.org/0009-0002-8451-3948

Pham Thai Gia Phu was on Feb 01st, 2001. He is student in Faculty of Applied Sciences, Ho Chi Minh City University of Technology and Education. His thesis is gold nanostars and investigation their photothermal effect.
Email: 19130040@student.hcmute.edu.vn. ORCID: https://orcid.org/0009-0005-2115-0387

Nguyen Thi Hong Tham is Ph.D. student in Physics and Engineering Physics Faculty of University of Science, VNUHCM. She received B.S. degree (2012) and M.S. degree (2017) in Faculty of Materials Science and Technology, University of Science, VNUHCM. From 2015 to now (2023), she is the researcher at Semiconductor Laboratory, Laboratories of Saigon Hi-tech Park. Her research focuses on using deep learning in characterizing noble metallic nanoparticles.
Email: nththam.shtp@tphcm.gov.vn. ORCID: https://orcid.org/0009-0006-5257-7604